Spatial and temporal variation of PM 2.5 and PM 10 in cities in China from 2016 to 2018

Mingtao Chen
Guilin University of Technology
Qi Feng
Guilin University of Technology
Xing Gao
Guilin University of Technology
Hongqiang Wang (sjhjgc@163.com)
Guilin University of Technology
Lei Liao
Guilin University of Technology

Research Article

Keywords: PM2.5, PM10, Spatiotemporal characteristics

Posted Date: October 3rd, 2022

DOI: https://doi.org/10.21203/rs.3.rs-2094369/v1

Abstract

Particulate matter pollution is the cause of many diseases and the focus of urban atmospheric environmental research. Here, the spatiotemporal variations of $PM_{2.5}$ and PM_{10} concentrations were analyzed across 71 cities in China using spatiotemporal sequence analyses and spatial interpolation of national monitoring data collected between 2016 and 2018. Significant differences were observed in the spatiotemporal variations of $PM_{2.5}$ and PM_{10} concentrations across the country. $PM_{2.5}$ concentrations in winter, spring, autumn, and summer were 60.16, 41.95, 37.10, and 26.94 μg/m^3, respectively. The PM_{10} concentrations in spring and winter exhibited little difference at 89.50 and 92.30 μg/m^3, respectively, but were higher than values observed in autumn and summer. The national annual average $PM_{2.5}$ concentration decreased from 44.94 μg/m^3 in 2016 to 37.75 μg/m^3 in 2018, while that of PM_{10} decreased from 80.42 to 70.14 μg/m^3. From 2016 to 2018, the monthly average concentrations of $PM_{2.5}$ and PM_{10} in the 71 cities generally showed a downward trend. The average $PM_{2.5}$ concentration in May comprised a single yearly peak, while the average PM_{10} concentration in October exhibited a second peak. The national $PM_{2.5}$ and PM_{10} concentrations began to rise in September and October of each year and then decline in March and April of the next year. Spatial variation analysis revealed that the Hu Huanyong line is the east-west boundary line differentiating China's $PM_{2.5}$ and PM_{10} concentrations (excluding Xinjiang), while the Yangtze River is the north-south boundary line. High pollution areas were mainly distributed in fast-growing urban agglomerations for instance the Central Plains, Bohai, and Yangtze River Delta urban agglomerations, in addition to the Xinjiang region. The annual average $PM_{2.5}$ mass concentrations across the seven geographic regions of China followed the order of Central > North > Northwest > Northeast > East > Southwest > South China. Further, the annual average PM_{10} mass concentration followed the order of Northwest > Central > North > Northeast > North > Southwest > South China. From a spatial perspective, the $PM_{2.5}$ and PM_{10} concentrations began to rise in September and October every year, then gradually spread outward from the Shandong, Shanxi, Henan, and Hebei provinces. The monthly increases comprised about 10–20 μg/m^3, while the $PM_{2.5}$ average concentration in most areas south of the Yangtze River exceeded 60 μg/m^3 in May. Further, from March and April of the next year, a high-value area centered around Henan began to gradually decrease, and the division of concentrations between the north and south via the Yangtze River became more obvious.

Introduction

The acceleration of industrialization and urbanization in the past few decades has led to increasing levels of pollutants being emitted alongside considerable energy consumption, and these processes have seriously affected the quality of China’s atmospheric environments (Gurjar et al., 2016; Zhang et al., 2018). Fine air particles can introduce toxic and harmful substances into human respiratory tracts. Further, introduction into human bodies through the respiratory tract can induce cardiovascular system, blood system, and reproductive system diseases such as pharyngitis, asthma, rhinitis, lung cancer, and others (Buonanno et al., 2013; III et al., 2002; Kreyling et al., 2006; Pope Iii et al., 2002). Moreover, the risk

of lung cancer caused by ultrafine particles is much higher than that due of coarse particles(Li et al., 2022a). Consequently, fine air particles have been listed by cancer research institutions as human carcinogens (Buonanno et al., 2013). Preliminary studies have indicated that about 40% of cardiovascular and cerebrovascular diseases, in addition to 20% of lung cancer deaths in China can be attributed to aerosol pollution (Donkelaar et al., 2010). Further, other studies have shown that $PM_{2.5}$ and PM_{10} particles in the air contain abundant toxic substances that can pass through the respiratory system and cause direct harm to human health (Buonanno et al., 2013; Cesaroni et al., 2013; Liao et al., 2011). Moreover, the probability of lung cancer caused by $PM_{2.5}$ and PM_{10} is significantly higher than from coarse particles. Consequently, cancer research institutions have listed $PM_{2.5}$ and PM_{10} as human carcinogens. Cities exhibit the most serious $PM_{2.5}$ and PM_{10} pollution in China and these impacts extend to surrounding areas(Yan et al., 2018). In particular, the haze caused by increased $PM_{2.5}$ and PM_{10} concentrations is widespread in the Beijing-Tianjin-Hebei region, the Yangtze River Delta, the Pearl River Delta, and Northeast China, seriously limiting the sustainable development of these regional economies(Wang et al., 2021). Increasingly studies have shown that atmospheric particles produced by anthropogenic activities considerably impact regional air quality and global climate change (Racherla et al., 2006; Xue et al., 2019; Zhang et al., 2017). Therefore, investigating aerosol pollution problems in cities and their surrounding areas is an important area of focus.

Materials And Methods

Data sources

Data used in this study comprise hourly real-time data from national air quality automatic monitoring stations. The annual average value encompasses at least 324 daily average concentration values throughout the year according to the effectiveness requirements of the Ambient Air Quality Standard (GB3095-2012). The monthly average value encompasses at least 27 daily average concentration values every month (at least 25 daily average concentration values in February). Finally, daily average values encompass at least 20 hours of average concentration monitoring values or sampling times from every day. The data period encompassed by this study covers from January 1, 2016, to December 30, 2018. The implementation plan for the third stage of monitoring the new air quality standard for the Ministry of Environmental Protection incorporates monitoring points in 71 cities. Consequently, the dataset used here encompasses data from 71 cities (Fig. 1). A total of 426 monitoring stations are under state control for monitoring air quality.

The "daily average" was calculated as the arithmetic means of the 24-hour pollutant concentration at the station for a day, while the "monthly average" is the arithmetic mean of the daily pollutant concentration at a station in a calendar month, and the "quarterly average" is the arithmetic mean of the daily pollutant concentration of the station in a calendar quarter, as based on standards of ambient air quality (GB3095-2012). "Annual average value" refers to the arithmetic mean value of pollutant concentrations for each day at each station in a calendar year. Seasonal years were considered as the standard in this study and

included March to May as spring, June to August as summer, September to November as autumn, and December through February of the next year as winter.

Spatial interpolation

The $PM_{2.5}$ and PM_{10} concentrations are similar to state quantities such as air temperature, such that the $PM_{2.5}$ and PM_{10} concentrations are statistically close in similar areas. The complete spatial distribution in the region can thus be obtained by interpolation. Some studies have indicated that the accuracy of remote sensing inversion is not as accurate as a regional interpolation (Seung-Jae et al., 2012). Commonly used interpolation methods at regional scales include the Inverse Distance Weighted (IDW) and Kriging methods. The accuracy of the former estimated pixel is greatly affected by its distance to a known point and requires high dispersion and uniformity of interpolation points. However, the interpolation results of non-equilibrium interpolation points exhibit high volatility and poor continuity. The latter method conducts a comprehensive calculation of the spatial behavior of interpolated point attributes before generating a best estimation method for the output surface, resulting in better continuity of results (Ahmad et al., 2021; Gong et al., 2014; Zhang et al., 2013). In this study, the cross-validation method is used to verify that the Kriging accuracy is above 85%, which is better than IDW, so that the Kriging interpolation can be selected.

Results And Analysis

Analysis of aerosol temporal dynamics

The quality of China's atmospheric environment is poor according to the bulletin of China's ecological environment from 2016 to 2018. In 2016, only 84 cities nationwide exhibited ambient air quality that reached the standard, comprising 24.9% of all cities. Further, heavy pollution occurred a total of 2,464 times in cities across the country, of which 80.3% occurred due to $PM_{2.5}$ and 20.4% due to PM_{10}. In 2017, 29.3% of China's urban ambient air quality measurements reached the standard, while the proportion of $PM_{2.5}$ as the primary pollutant decreased to 74.2%, and the proportion of PM_{10} as the primary pollutant was the same as in 2016. The ambient air quality in 2018 improved compared with 2016 and 2017, with 35.8% of urban ambient air quality measurements reaching the standard, the proportion of $PM_{2.5}$ as the primary pollutant decreasing to 60.0%, and the proportion of PM_{10} as the primary pollutant increasing to 37.2%.

The $PM_{2.5}$ and PM_{10} concentration limits were the same as in the ambient air quality standard (GB3095-2012) (Table 1) and cities were divided into seven geographic regions (Table 2).

Table 1
$PM_{2.5}$ and PM_{10} concentration limits for standards

Contaminants	Averaging period	Concentration limit		Unit
		One-level	Second-level	
$PM_{2.5}$	Annual average	15	35	μg/m^3
	24 -hour average	35	75	
PM_{10}	Annual average	40	70	
	24 -hour average	50	150	

Table 2
Cities with data evaluated in this study and their corresponding geographic division

Geographic division	**City**
Northeast China	Harbin, Jiamusi, Changchun, Baicheng, Shenyang, Chaoyang
North China	Beijing, Tianjin, Hohhot, Alxa Left Banner, Hulunbuir, Shijiazhuang, Taiyuan, Datong, Changzhi
East China	Shanghai, Jinan, Jining, Weihai, Nanjing, Nantong, Lianyungang, Hangzhou, Lishui, Zhoushan, Hefei, Anqing, Suzhou, Fuzhou, Xiamen, Nanping, Nanchang
South China	Guangzhou, Shenzhen, Zhanjiang, Nanning, Beihai, Guilin, Haikou, Sanya
Central China	Zhengzhou, Xinyang, Sanmenxia, Wuhan, Jingzhou, Shiyan, Changsha, Zhangjiajie
Northwest China	Xi'an, Yan'an, Hanzhong, Urumqi, Kashgar, Altay, Haixi, Lanzhou, Jinchang, Yinchuan, Guyuan, Zhongwei
Southwest China	Chongqing, Xining, Guiyang, Tongren, Liupanshui, Chengdu, Ganzi, Kunming, Lijiang, Jinghong, Lhasa

Analysis of interannual $PM_{2.5}$ and PM_{10} variation among seven geographic regions of China

The interannual variation characteristics of $PM_{2.5}$ and PM_{10} across the country were determined using the hourly $PM_{2.5}$ and PM_{10} data from 71 cities between 2016 and 2018. The $PM_{2.5}$ and PM_{10} concentrations decreased year by year (Fig. 2). The national annual average concentration of $PM_{2.5}$ reduced from 44.94 to 37.75 μg/m^3, while the PM_{10} reduced from 80.42 to 70.14 μg/m^3 from 2016 to 2018. Thus, China's atmospheric environment improved after the implementation of the Ambient Air Quality Standard (GB3095-2012) on January 1, 2016. Even so, the annual average concentrations of $PM_{2.5}$ and PM_{10} could only barely reach the secondary concentration limit in 2018.

The data from each city were sorted and analyzed (Table 2) to assess the interannual changes in $PM_{2.5}$ and PM_{10} in each major geographic region between 2016 to 2018. The average annual $PM_{2.5}$ mass concentration from 2016 to 2018 (Fig. 3) followed the order of Central > North > Northwest > Northeast > East > Southwest > South China. In addition, the average annual PM_{10} mass concentration from 2016 to 2018 followed the order of Northwest > Central > North > Northeast > East > Southwest > South China. Querol et al.(2001; 2004) demonstrated that the $PM_{2.5}$ to PM_{10} concentration ratios greatly vary among different regions, although the $PM_{2.5}$ to PM_{10} concentration ratios in most areas are about 0.6–0.75 (Gehrig et al., 2003; Parkhurst et al., 1999). The ratio of $PM_{2.5}$ to PM_{10} concentrations in Northwest China was smaller than in central and northern China. However, South China encompasses the southern coast of China. In this area, ocean winds and the monsoon climate can increase the horizontal migration of aerosol particles on the surface, while clean air input at sea level can reduce the mass concentrations of aerosol particles.

Seasonal variation of $PM_{2.5}$ and PM_{10} in seven geographic regions of China

Statistical analysis of $PM_{2.5}$ and PM_{10} concentrations in 71 cities across China showed that the variation characteristics were generally high in spring and winter, and low in summer and autumn (Fig. 4). The $PM_{2.5}$ concentration was highest in winter, followed by spring, autumn, and summer, at 60.16, 41.95, 37.10, and 26.94 μg/m^3, respectively. PM_{10} concentrations in spring and winter exhibited little difference at 89.50 and 92.30 μg/m^3, respectively, which were higher than in autumn and summer.

Seasonal variations of $PM_{2.5}$ and PM_{10} concentrations in major geographic regions were evaluated (Fig. 5). From 2016 to 2018, the $PM_{2.5}$ concentration in winter was higher than in all other seasons, and even the concentration in winter was 2–3 times higher than that in summer. Wind speed, relative humidity, and precipitation in winter were lower than in other seasons. In addition, winter exhaust gas emissions from heating in northern China are high(Fan et al., 2020). Further, the coverage of green plants decreases in winter, and their consequent removal effects on pollutants decrease. The $PM_{2.5}$ concentration in Central China was much higher than in other regions in winter, while in summer, the $PM_{2.5}$ concentration in North China was the highest. Central, Northwest, and East China exhibited essentially the same trends, while Northeast, Southwest, and South China exhibited the lowest concentrations. Northeast and South China are relatively close to the ocean, and the prevailing hot and humid atmosphere blows inland from June to August, thereby greatly reducing $PM_{2.5}$ concentrations in those regions. The $PM_{2.5}$ concentration in spring and autumn had little difference among regions, while the $PM_{2.5}$ concentration in the spring of Northwest China was above 25% higher than in autumn. From 2016 to 2018, PM_{10} concentrations were different from $PM_{2.5}$, with no single season exhibiting higher values than the other seasons. North, Northwest, and Northeast China, the PM_{10} concentration was

highest in the spring, followed by the winter, autumn, and summer, while the seasonal variations of the other four regions were similar to $PM_{2.5}$.

Annual variation of $PM_{2.5}$ and PM_{10} concentrations in seven geographic regions of China

The monthly average concentrations of $PM_{2.5}$ and PM_{10} in 71 cities nationwide showed a downward trend from 2016 to 2018 (Fig. 6). The annual change trends for $PM_{2.5}$ were relatively stable. From January to August, the monthly average $PM_{2.5}$ concentration in 71 cities across the country gradually decreased, and then increased from September to December. The monthly average concentrations of PM_{10} were different from $PM_{2.5}$, with two peaks that were observed yearly in March and December, respectively.

PM_{10} concentrations exhibited a sharp decreasing trend from March to June every year but rose sharply from October to December. The reasons underlying the sharp increase of PM_{10} and $PM_{2.5}$ concentrations from October to December are two-fold. First, the temperature begins to decrease in October and the sinking of cold air decreases the diffusion of $PM_{2.5}$ and PM_{10} in the atmosphere. Reduced rainfall also decreases wet deposition. Heating gradually increases in northern cities at this time and this fuel combustion is accompanied by the direct emission of particulate matter, while also producing SO_2, NO_2, and other noxious gases that provide a foundation for $PM_{2.5}$ and PM_{10} generation, resulting in sharply increased concentrations of PM_{10} and $PM_{2.5}$ from October to December(Hallquist et al., 2009).

The PM_{10} concentrations sharply decreased from March to June every year, while $PM_{2.5}$ concentrations gradually decreased. National temperatures began to rise in March, coinciding with diminishing northern heating. The different trends of $PM_{2.5}$ and PM_{10} concentration variations may be related to the rainy season that begins in March. Different rainfall, rainfall intensity, and rainfall lengths lead to different effects on the removal of atmospheric particulate matter of different particle sizes. Most of the rainfall between March to June is characterized by low rainfall intensity and long rainfall times.

Based on the above analyses, variations in the annual $PM_{2.5}$ and PM_{10} concentrations or seven geographic regions were evaluated (Fig. 7). PM_{10} concentrations throughout the country increase to varying extents from October to December, and climate conditions considerably impact PM_{10} concentrations. However, increased PM_{10} concentrations between October to December were more obvious in North, Central, and Northwest China compared to within East, South, and Southwest China, reflecting that urban heating in the north influences PM10 concentrations across those cities. $PM_{2.5}$ concentrations in Central China increased most significantly from October to December.

Aerosol spatial variation

Daily $PM_{2.5}$ and PM_{10} data from 2016 to 2018 at an hourly resolution were averaged to obtain spatial distribution visualizations for $PM_{2.5}$ and PM_{10} concentrations (Figs. 8 and 9). Areas with high annual average concentrations of $PM_{2.5}$ and PM_{10} were mainly in the Beijing-Tianjin-Hebei, Jianghuai Plain, and Xinjiang regions, where annual average concentrations of $PM_{2.5}$ were above 70 μg/m^3.

High-pollution areas were primarily distributed in rapidly developing urban agglomerations such as the Central Plains, the Bohai Sea, and the Yangtze River Delta urban agglomerations. The rapid development of industries and urban construction in these areas have led to sharp increases in $PM_{2.5}$ and PM_{10} concentrations. Meanwhile, these urban agglomerations are also densely populated areas in China. Human activities and the development of urban infrastructures including motor vehicles, heating in winter, and infrastructure construction have all contributed to increased air pollution(Li et al., 2022b).

The overall terrain of China is high in the west and low in the east, and the local topography is complex and diverse. Landforms such as plateaus, basins, and hills are not conducive to pollutant diffusions. The concentrations of $PM_{2.5}$ and PM_{10} in Xinjiang are relatively high due to the effects of terrain factors, such as the flowing dunes in the Tarim Basin. When windy and dusty weather occurs, pollutants cannot be evacuated due to the terrain, thereby greatly increasing local $PM_{2.5}$ and PM_{10} concentrations.

Areas with low $PM_{2.5}$ and PM_{10} concentrations were primarily distributed in South China, the Qinghai-Tibet Plateau, and the Yunnan-Guizhou region. The Qinghai-Tibet Plateau is considered the pure land of China's environment. The plateau exhibits high altitudes and is also sparsely populated. The Yunnan-Guizhou region and South China exhibit considerable rainfall, lush green plants, and obvious monsoon climates that play an active part in the migration and purification of pollutants, so the air quality is better than in other regions.

Seasonal spatial characteristics

From 2016 to 2018, $PM_{2.5}$ and PM_{10} concentrations in the spring, summer, autumn, and winter exhibit obvious seasonal changes that can be observed in Figs. 10 and 11. The concentrations of $PM_{2.5}$ and PM_{10} were highest in the winter, followed by the spring and autumn, and then lowest in the summer. Seasonal variation of $PM_{2.5}$ and PM_{10} concentrations are mainly affected by human activities and meteorological factors(Li et al., 2017). For example, at the beginning of autumn, $PM_{2.5}$ and PM_{10} concentrations in the Bohai-rim urban agglomeration gradually rise, resulting in the onset of high pollution areas in the Shandong, Shanxi, Henan, and Hebei provinces that continue until winter, while in spring $PM_{2.5}$ and PM_{10} concentrations begin to decrease.

$PM_{2.5}$ and PM_{10} pollution were the most serious in winter, and the distribution range was also the widest. The $PM_{2.5}$ concentrations mostly ranged from 70 to 130 μg/m^3, while the PM_{10} concentrations mostly ranged from 150 to 200 μg/m^3. Two primary reasons underlie this phenomenon. First, exhaust gas emissions are large during heating periods for cities in northern China. Second, green plant coverage is

low during winter and the dilution of pollutants is reduced, leading to higher $PM_{2.5}$ and PM_{10} concentrations than in other seasons.

The $PM_{2.5}$ and PM_{10} concentrations decreased in autumn relative to winter, with $PM_{2.5}$ concentrations decreasing to 35–60 μg/m^3 in the area of 70–130 μg/m^3 and spreading to the north. Relative to winter levels, the $PM_{2.5}$ and PM_{10} concentrations in South China were significantly decreased, which may be related to typhoons and wetter climates.

Summer seasons exhibited the lowest $PM_{2.5}$ and PM_{10} concentrations and the best air quality. The $PM_{2.5}$ and PM_{10} concentrations in summer were significantly lower than in autumn and winter. Specifically, $PM_{2.5}$ concentrations ranged between 15 and 30 μg/m^3 in most areas, and PM_{10} concentrations ranged between 20 and 55 μg/m^3, with higher values appearing in northern areas. The high level of air quality in the summer arises primarily because ocean winds prevail in China from June to August. Ocean winds blow hot and humid air over the ocean to the land which can then greatly reduce $PM_{2.5}$ and PM_{10} concentrations. However, PM_{10} concentrations in Xinjiang, in addition to $PM_{2.5}$ concentrations on the eastern coast exhibited high values that were primarily related to the topography of China.

Areas in the northern region still use heating in the spring, and thus, the high-value areas of $PM_{2.5}$ and PM_{10} concentrations in the northern region are more significant than in the south, although areas with low concentrations in the north are lesser than those of the summer. $PM_{2.5}$ concentrations increased to 50–90 μg/m^3, and PM_{10} concentrations increased to 90–150 μg/m^3.

Monthly spatial characteristics

Areas with high monthly average concentrations of $PM_{2.5}$ and PM_{10} appeared around Henan and northwestern Xinjiang from January 2016 to 2018 (Figs. 12 and 13). In most areas of Henan, the monthly average concentration of $PM_{2.5}$ reached 100 μg/m^3 and the monthly average concentration of PM_{10} reached 140 μg/m^3, and these improved in February. The monthly average $PM_{2.5}$ concentrations in high-value areas centered around Henan generally decreased by 20–30 μg/m^3, while the monthly average PM_{10} concentration decreased by 30–40 μg/m^3. Except for two high-value areas, the monthly average PM_{10} concentrations in most areas of the country were below 70 μg/m^3, while the monthly average $PM_{2.5}$ concentrations were below 50 μg/m^3. Beginning in March, the high-value area centered around Henan gradually weakened, and a development trend appeared to the north. The air quality in the south improved due to the onset of the rainy season. The average monthly $PM_{2.5}$ concentrations in the Fujian and Zhejiang provinces were below 35 μg/m^3.

Nationwide air quality improved in April and May, which was directly related to the end of heating use in northern cities. The regions with higher values included Shandong, Shanxi, Henan, and Hebei. These provinces are concentrated in areas of China with heavy industry and have relatively dense populations. The air quality in the southern provinces has improved significantly, considering the Yangtze River as the

dividing line for the country. The monthly average $PM_{2.5}$ concentrations were lower than 35 μg/m^3 and the monthly average PM_{10} concentrations were lower than 60 μg/m^3. Similar observations were made from June to August, with high $PM_{2.5}$ values in Xinjiang decreasing. In these three months, high-value areas appeared in the Bohai-rim urban agglomeration, the Jianghuai Plain, and the Fenwei Plain. The average $PM_{2.5}$ concentrations in the south and west of the Yangtze River were lower than 30 μg/m^3. After clearing by the marine monsoon climate from June to August, the monthly average PM_{10} concentrations in most parts of China were lower than 70 μg/m^3.

A $PM_{2.5}$ high-value area in Xinjiang began to appear in September, and the monthly average $PM_{2.5}$ concentration in the south of the Yangtze River also increased. The monthly average PM_{10} concentrations also generally increased by 10–20 μg/m^3 nationwide. $PM_{2.5}$ and PM_{10} high-value areas centered around Hebei began to appear in September, while $PM_{2.5}$ and PM_{10} concentrations increased throughout the country. High-value areas centered around the Shandong, Shanxi, Henan, and Hebei provinces gradually became obvious from November to December. By December, the average concentration of $PM_{2.5}$ in most areas south of the Yangtze River exceeded 60 μg/m^3.

Conclusions

China's atmospheric environment has improved to a certain extent since the implementation of the Ambient Air Quality Standard (GB3095-2012) on January 1, 2016. The national average annual concentration of $PM_{2.5}$ dropped from 44.94 μg/m^3 in 2016 to 37.75 μg/m^3 in 2018, while PM_{10} concentrations decreased from 80.42 to 70.14 μg/m^3 in the same period.

Spatial distribution analysis revealed that the Heihe-Tengchong Line is the east-west boundary of $PM_{2.5}$ and PM_{10} concentrations in China (excluding the Xinjiang region), while the Yangtze River is the north-south division boundary. High-pollution areas were mainly distributed in fast-growing urban agglomerations including the Central Plains, Bohai, and Yangtze River Delta urban agglomerations, as well as the Xinjiang region. The annual average $PM_{2.5}$ mass concentrations in the seven geographic regions of China followed the order of Central > North > Northwest > Northeast > East > Southwest > South China. Further, the annual average PM_{10} mass concentrations in the regions followed the order of Northwest > Central > North > Northeast > North > Southwest > South China.

The monthly average concentrations of $PM_{2.5}$ and PM_{10} in 71 cities across the country generally decreased from 2016 to 2018. The monthly average $PM_{2.5}$ concentrations exhibited a single peak, while the monthly average PM_{10} concentrations exhibited two peaks. In September and October of each year, the national $PM_{2.5}$ and PM_{10} concentrations began to rise but then declined in March and April of the following year. From a spatial perspective, the $PM_{2.5}$ and PM_{10} concentrations begin to rise in September and October every year and gradually spread outward from the Shandong, Shanxi, Henan, and Hebei provinces, increasing by about 10–20 μg/m^3 per month. The monthly average concentration of PM2.5 in

most areas south of the Yangtze River exceeded 60 μg/m^3. In March and April of the following year, a high-value area centered around Henan began to gradually decrease and the division between the north and south of the Yangtze River became more obvious.

Declarations

Funding The work was supported by the Youth Fund of Guangxi Natural Science Foundation (NO.2018GXNSFBA281082).

Data availability All necessary data are included in the document.

Conflict of interest The authors declare no competing interests.

Author Contributions Statement Hongqiang Wang and Lei Liao conceived and designed the research, interpreted, analyzed, and discussed the obtained data. Mingtao Chen, Qi Feng, and Xing Gao wrote the manuscript and all authors commented on previous versions of the manuscript. Finally, all authors reviewed the manuscript.

Acknowledgments We thank LetPub (www.letpub.com) for this linguistic assistance during the preparation of this manuscript

References

1. Ahmad, A. Y., Saleh I. A., Balakrishnan P.&Al-Ghouti M. A. (2021). Comparison GIS-Based interpolation methods for mapping groundwater quality in the state of Qatar. Groundwater for Sustainable Development, *13*, 100573. https://doi.org/10.1016/j.gsd.2021.100573
2. Buonanno, G., Marks G. B.&Morawska L. (2013). Health effects of daily airborne particle dose in children: Direct association between personal dose and respiratory health effects. Environmental Pollution, *180*, 246–250. https://doi.org/10.1016/j.envpol.2013.05.039
3. Cesaroni, G., Badaloni C., Gariazzo C., Stafoggia M., Sozzi R., Davoli M.&Forastiere F. (2013). Long-term exposure to urban air pollution and mortality in a cohort of more than a million adults in Rome. Environmental Health Perspectives, *121*(3), 324–331. https://doi.org/10.1289/ehp.1205862
4. Donkelaar, A. v., Martin a. V., Brauer M., Kahn R., Levy R., Verduzco C.&Villeneuve P. J. (2010). Global Estimates of Ambient Fine Particulate Matter Concentrations from Satellite-Based Aerosol Optical Depth: Development and Application. Environmental Health Perspectives, *118*(6), 847–855. https://doi.org/10.1289/ehp.0901623
5. Fan, M., He G.&Zhou M. (2020). The winter choke: Coal-Fired heating, air pollution, and mortality in China. Journal of Health Economics, *71*, 102316. https://doi.org/10.1016/j.jhealeco.2020.102316
6. Gehrig, R.&Buchmann B. (2003). Characterising seasonal variations and spatial distribution of ambient PM10 and PM2.5 concentrations based on long-term Swiss monitoring data. Atmospheric Environment, *37*(19), 2571–2580. https://doi.org/10.1016/S1352-2310(03)00221-8

7. Gong, G., Mattevada S.&O'Bryant S. E. (2014). Comparison of the accuracy of kriging and IDW interpolations in estimating groundwater arsenic concentrations in Texas. Environmental Research, *130*, 59–69. https://doi.org/10.1016/j.envres.2013.12.005
8. Gurjar, B. R., Ravindra K.&Nagpure A. S. (2016). Air pollution trends over Indian megacities and their local-to-global implications. Atmospheric Environment, *142*, 475–495. https://doi.org/10.1016/j.atmosenv.2016.06.030
9. Hallquist, M., Wenger J. C., Baltensperger U., Rudich Y., Simpson D., Claeys M., Dommen J., Donahue N., George C.&Goldstein A. (2009). The formation, properties and impact of secondary organic aerosol: current and emerging issues. Atmospheric chemistry and physics, *9*(14), 5155–5236. https://doi.org/10.5194/acp-9-5155-2009
10. III, C. A. P., Burnett R. T., Thun M. J., Calle E. E., Krewski D., Ito K.&Thurston G. D. (2002). Lung Cancer, Cardiopulmonary Mortality, and Long-term Exposure to Fine Particulate Air Pollution. JAMA, *287*(9), 1132–1141. http://doi.org/10.1001/jama.287.9.1132
11. Kreyling, W. G., Semmler-Behnke M.&Möller W. (2006). Health implications of nanoparticles. Journal of Nanoparticle Research, *8*(5), 543–562. https://doi.org/10.1007/s11051-005-9068-z
12. Li, R., Cui L., Li J., Zhao A., Fu H., Wu Y., Zhang L., Kong L.&Chen J. (2017). Spatial and temporal variation of particulate matter and gaseous pollutants in China during 2014–2016. Atmospheric Environment, *161*, 235–246. https://doi.org/10.1016/j.atmosenv.2017.05.008
13. Li, S., Wang G., Geng Y., Wu W.&Duan X. (2022a). Lung function decline associated with individual short-term exposure to PM1, PM2.5 and PM10 in patients with allergic rhinoconjunctivitis. Science of the Total Environment, 158151. https://doi.org/10.1016/j.scitotenv.2022.158151
14. Li, W., Yang G.&Qian X. (2022b). The socioeconomic factors influencing the PM2.5 levels of 160 cities in China. Sustainable Cities and Society, *84*, 104023. https://doi.org/10.1016/j.scs.2022.104023
15. Liao, C.-M., Chio C.-P., Chen W.-Y., Ju Y.-R., Li W.-H., Cheng Y.-H., Liao V. H.-C., Chen S.-C.&Ling M.-P. (2011). Lung cancer risk in relation to traffic-related nano/ultrafine particle-bound PAHs exposure: A preliminary probabilistic assessment. Elsevier, *190*(1–3), 150–158. https://doi.org/10.1016/j.jhazmat.2011.03.017
16. Parkhurst, W. J., Tanner R. L., Weatherford F. P., Valente R. J.&Meagher J. F. (1999). Historic PM2. 5/PM10 concentrations in the southeastern United States—Potential implications of the revised particulate matter standard. Journal of the Air & Waste Management Association, *49*(9), 1060–1067. https://doi.org/10.1080/10473289.1999.10463894
17. Pope Iii, C. A., Burnett R. T., Thun M. J., Calle E. E., Krewski D., Ito K.&Thurston G. D. (2002). Lung cancer, cardiopulmonary mortality, and long-term exposure to fine particulate air pollution. JAMA, *287*(9), 1132–1141. https://doi.org/10.1001/jama.287.9.1132
18. Querol, X., Alastuey A., Rodriguez S., Plana F., Ruiz C. R., Cots N., Massagué G.&Puig O. (2001). PM10 and PM2.5 source apportionment in the Barcelona Metropolitan area, Catalonia, Spain. Atmospheric Environment, *35*(36), 6407–6419. https://doi.org/10.1016/S1352-2310(01)00361-2

19. Querol, X., Alastuey A., Ruiz C. R., Artiñano B., Hansson H. C., Harrison R. M., Buringh E., Brink H. M. t., Lutz M., Bruckmann P., Straehl P.&Schneider J. (2004). Speciation and origin of PM10 and PM2.5 in selected European cities. *Atmospheric Environment, 38*(38), 6547–6555. https://doi.org/10.1016/j.atmosenv.2004.08.037
20. Racherla, P. N.&Adams P. J. (2006). Sensitivity of global tropospheric ozone and fine particulate matter concentrations to climate change. Journal of Geophysical Research: Atmospheres, *111*(D24), https://doi.org/10.1029/2005JD006939
21. Seung-Jae, L., L S. M., Aaron v. D., V M. R., T B. R.&Michael J. (2012). Comparison of geostatistical interpolation and remote sensing techniques for estimating long-term exposure to ambient PM2.5 concentrations across the continental United States. Environmental Health Perspectives, *120*(12), 1727–1732. https://doi.org/10.1289/ehp.1205006
22. Wang, J., Li R., Xue K.&Fang C. (2021). Analysis of Spatio-Temporal Heterogeneity and Socioeconomic driving Factors of PM2.5 in Beijing–Tianjin–Hebei and Its Surrounding Areas. Atmosphere, *12*(10), 1324. https://doi.org/10.3390/atmos12101324
23. Xue, H., Liu G., Zhang H., Hu R.&Wang X. (2019). Similarities and differences in PM10 and PM2.5 concentrations, chemical compositions and sources in Hefei City, China. Chemosphere, *220*, 760–765. https://doi.org/10.1016/j.chemosphere.2018.12.123
24. Yan, D., Lei Y., Shi Y., Zhu Q., Li L.&Zhang Z. (2018). Evolution of the spatiotemporal pattern of PM2.5 concentrations in China – A case study from the Beijing-Tianjin-Hebei region. Atmospheric Environment, *183*, 225–233. https://doi.org/10.1016/j.atmosenv.2018.03.041
25. Zhang, A., Qi Q., Jiang L., Zhou F.&Wang J. (2013). Population exposure to PM2.5 in the urban area of Beijing. PloS one, *8*(5), 1–9. https://doi.org/10.1371/journal.pone.0063486
26. Zhang, H., Yuan H., Liu X., Yu J.&Jiao Y. (2018). Impact of synoptic weather patterns on 24 h-average PM 2.5 concentrations in the North China Plain during 2013–2017. Science of the Total Environment, *627*, 200–210. https://doi.org/10.1016/j.scitotenv.2018.01.248
27. Zhang, M., Zhang S., Feng G., Su H., Zhu F., Ren M.&Cai Z. (2017). Indoor airborne particle sources and outdoor haze days effect in urban office areas in Guangzhou. Environmental Research, *154*, 60–65. https://doi.org/10.1016/j.envres.2016.12.021

Figures

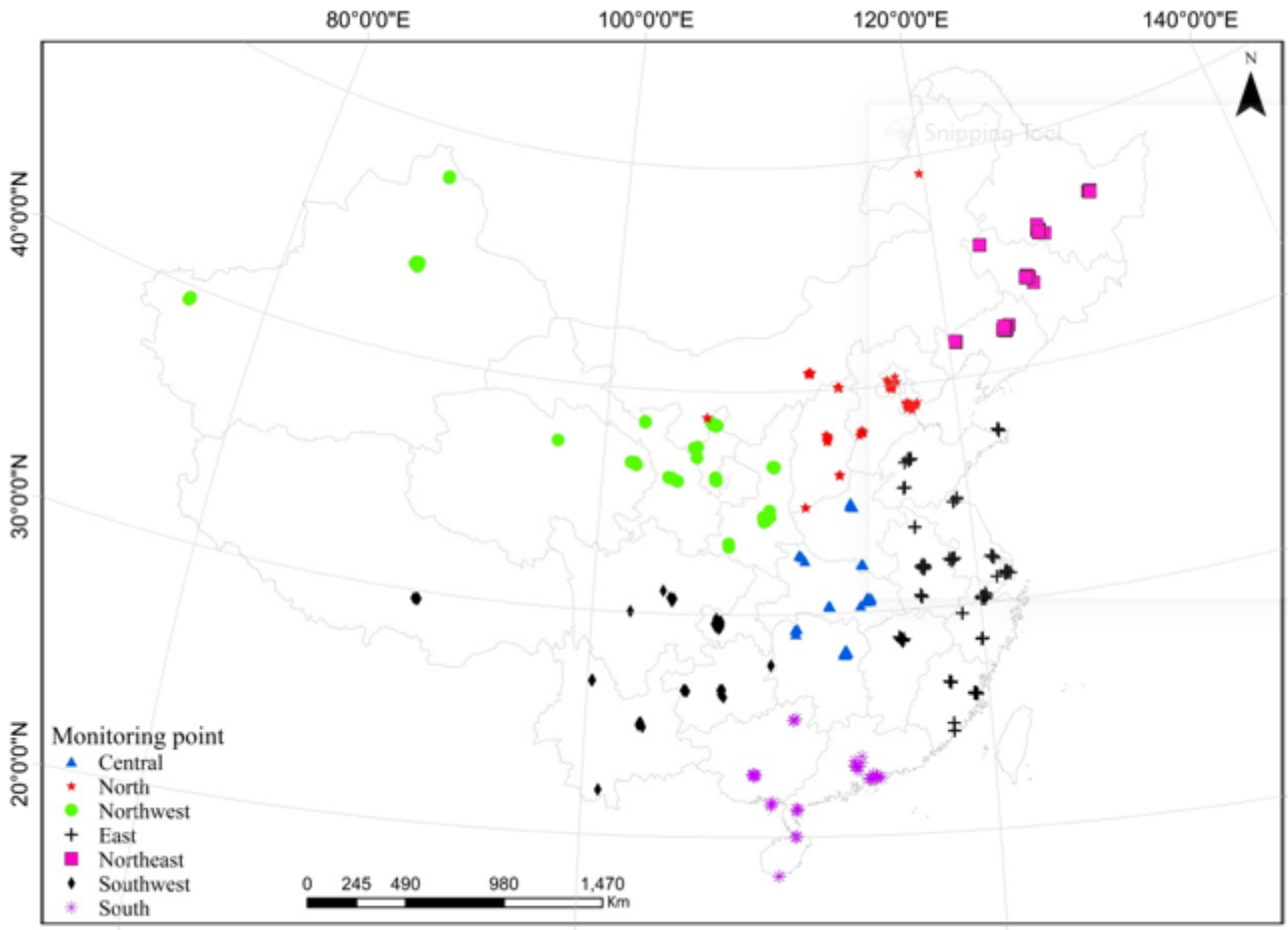

Figure 1

Map of monitoring points in 71 cities in China

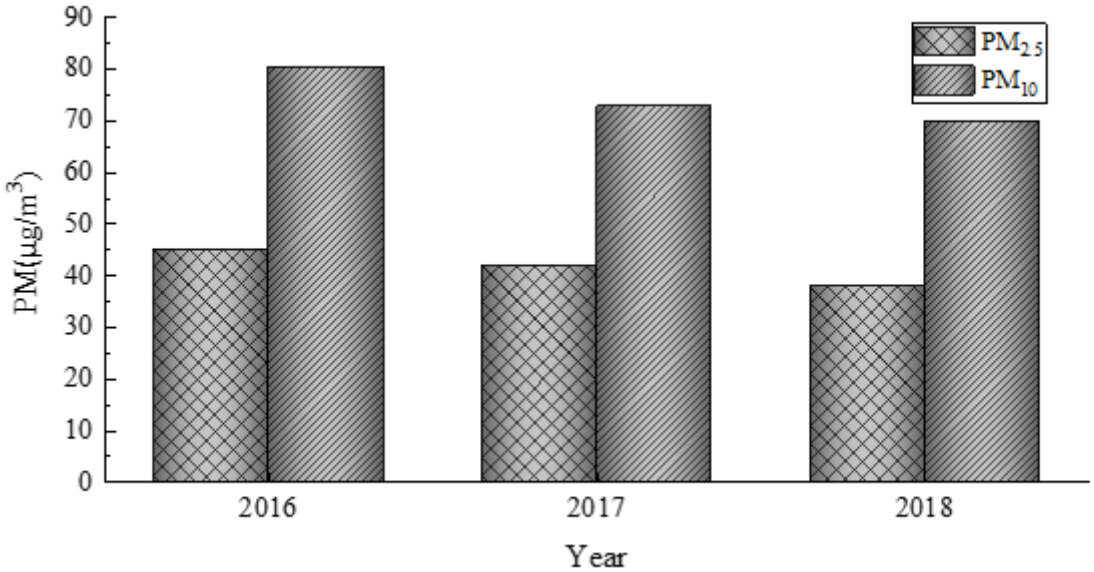

Figure 2

National annual average concentrations of $PM_{2.5}$ and PM_{10} in China from 2016 to 2018

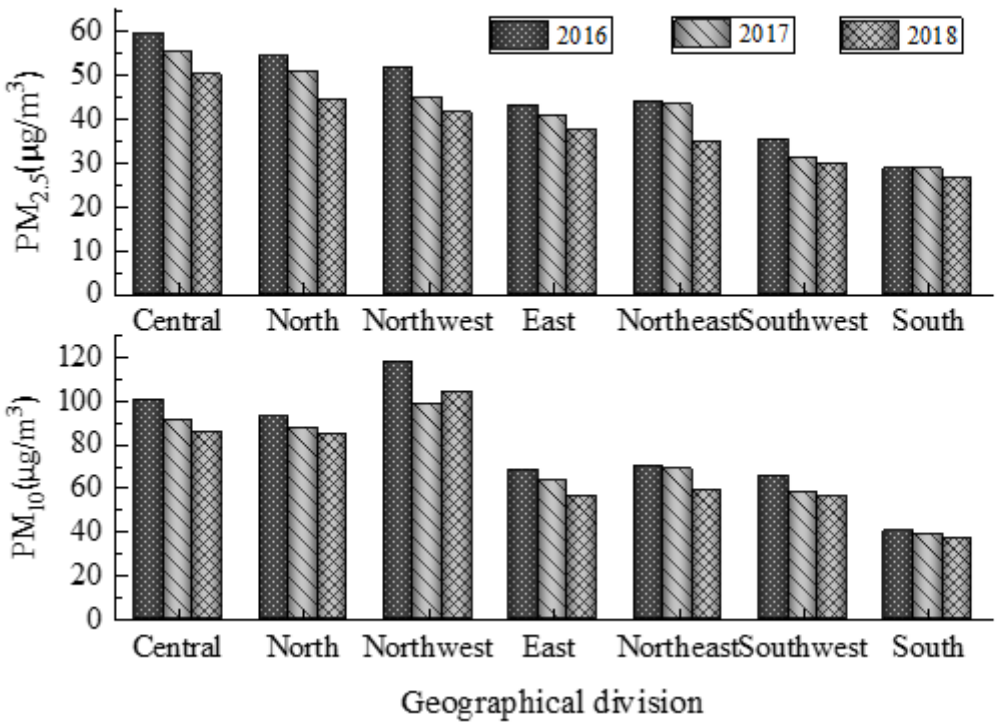

Figure 3

Annual average concentrations of $PM_{2.5}$ and PM_{10} in seven geographical regions of China from 2016 to 2018

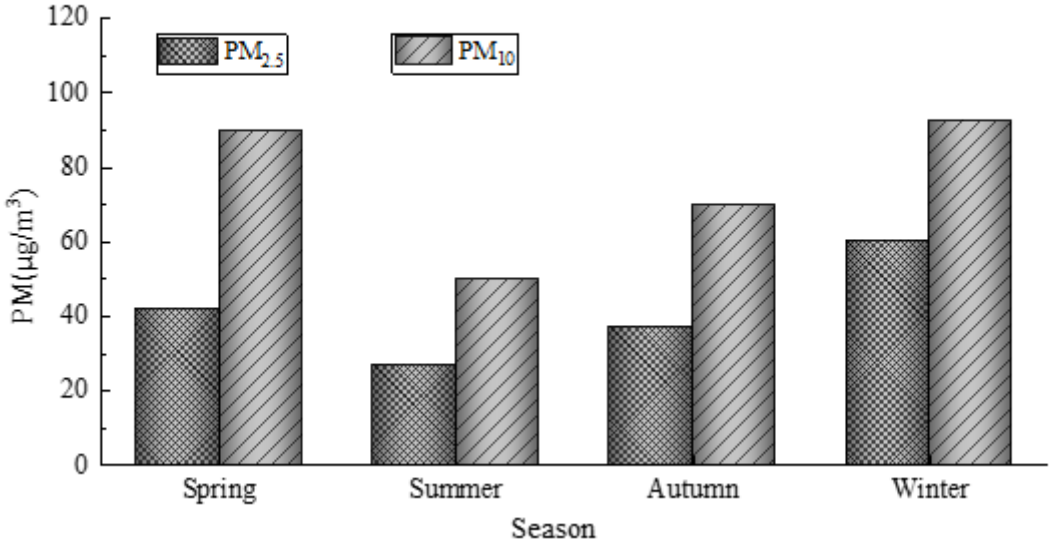

Figure 4

Average seasonal concentrations of $PM_{2.5}$ and PM_{10} in China between 2016 and 2018

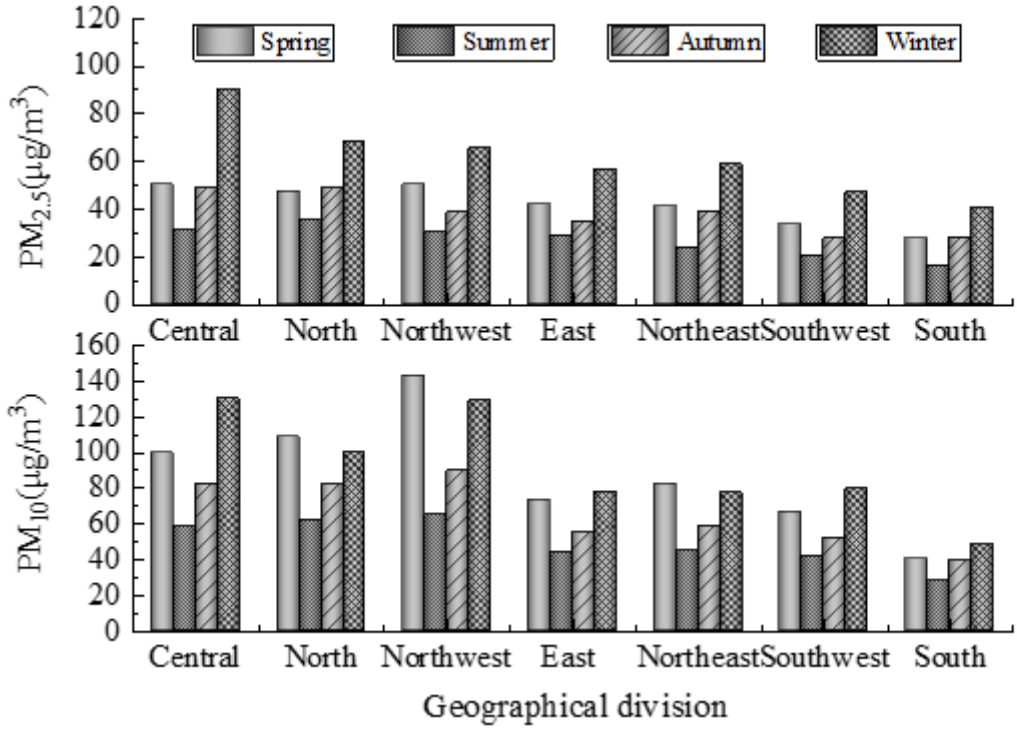

Figure 5

Seasonal average concentrations of $PM_{2.5}$ and PM_{10} in seven geographic regions of China from 2016 to 2018

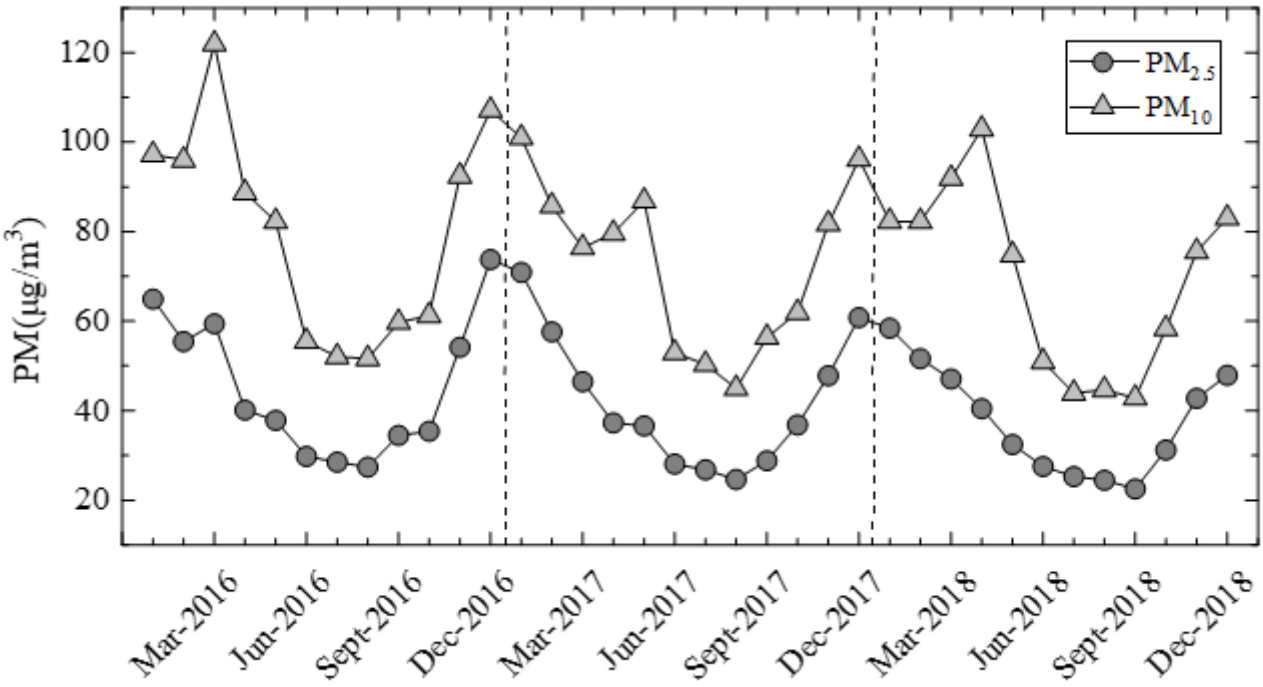

Figure 6

National monthly average $PM_{2.5}$ and PM_{10} concentrations from 2016 to 2018

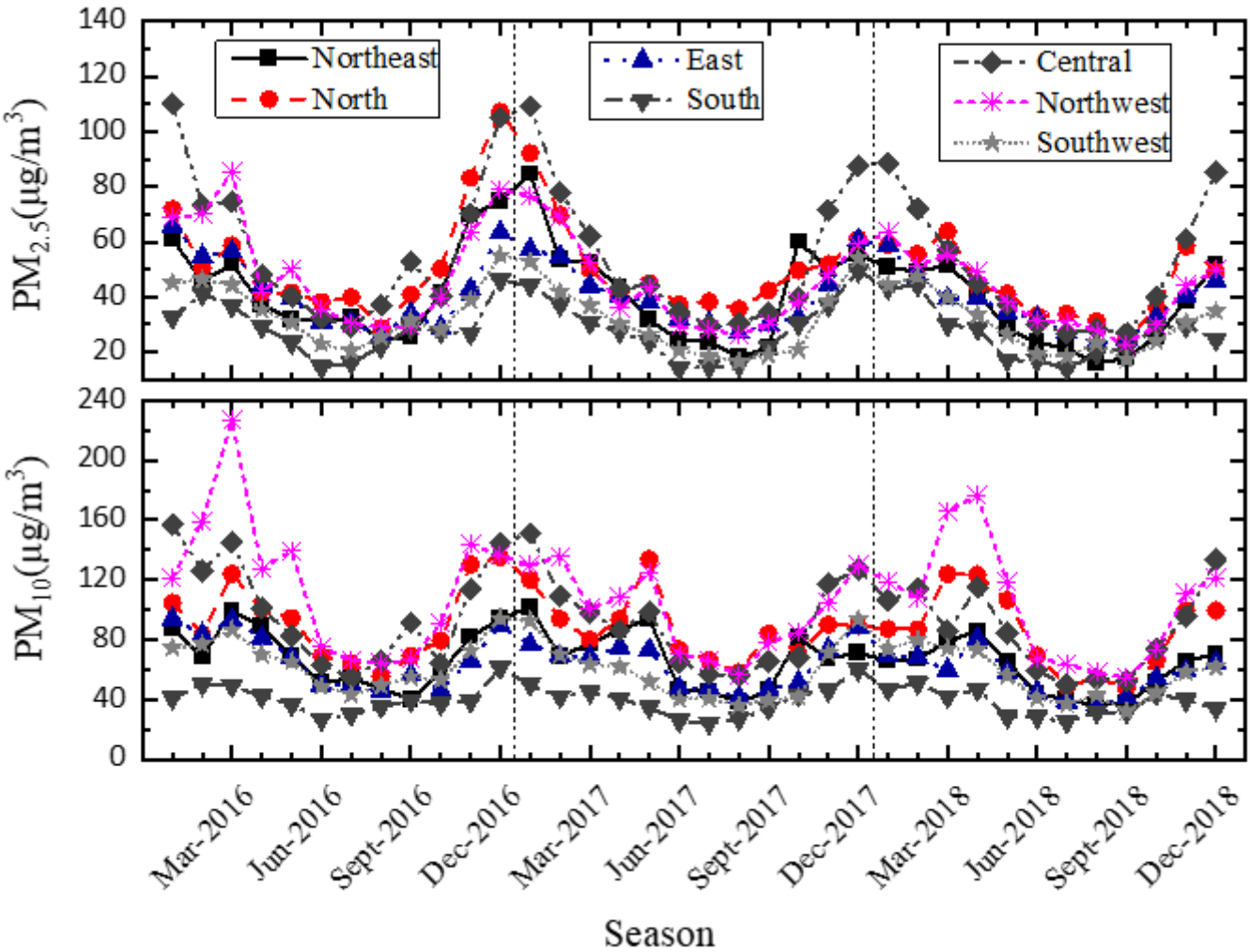

Figure 7

Monthly average $PM_{2.5}$ and PM_{10} concentrations among seven geographic regions from 2016 to 2018

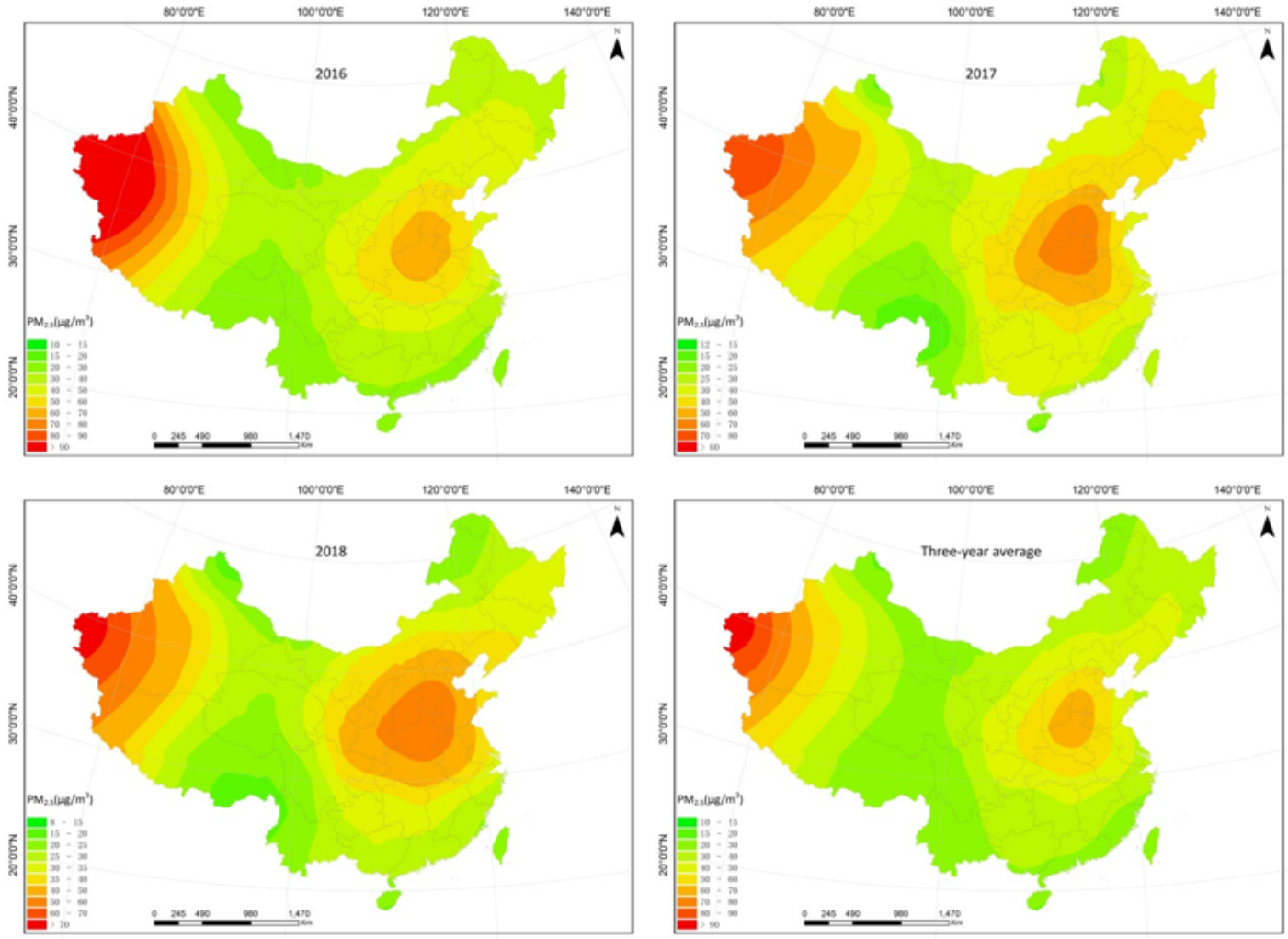

Figure 8

Spatial distribution of $PM_{2.5}$ concentrations from 2016 to 2018

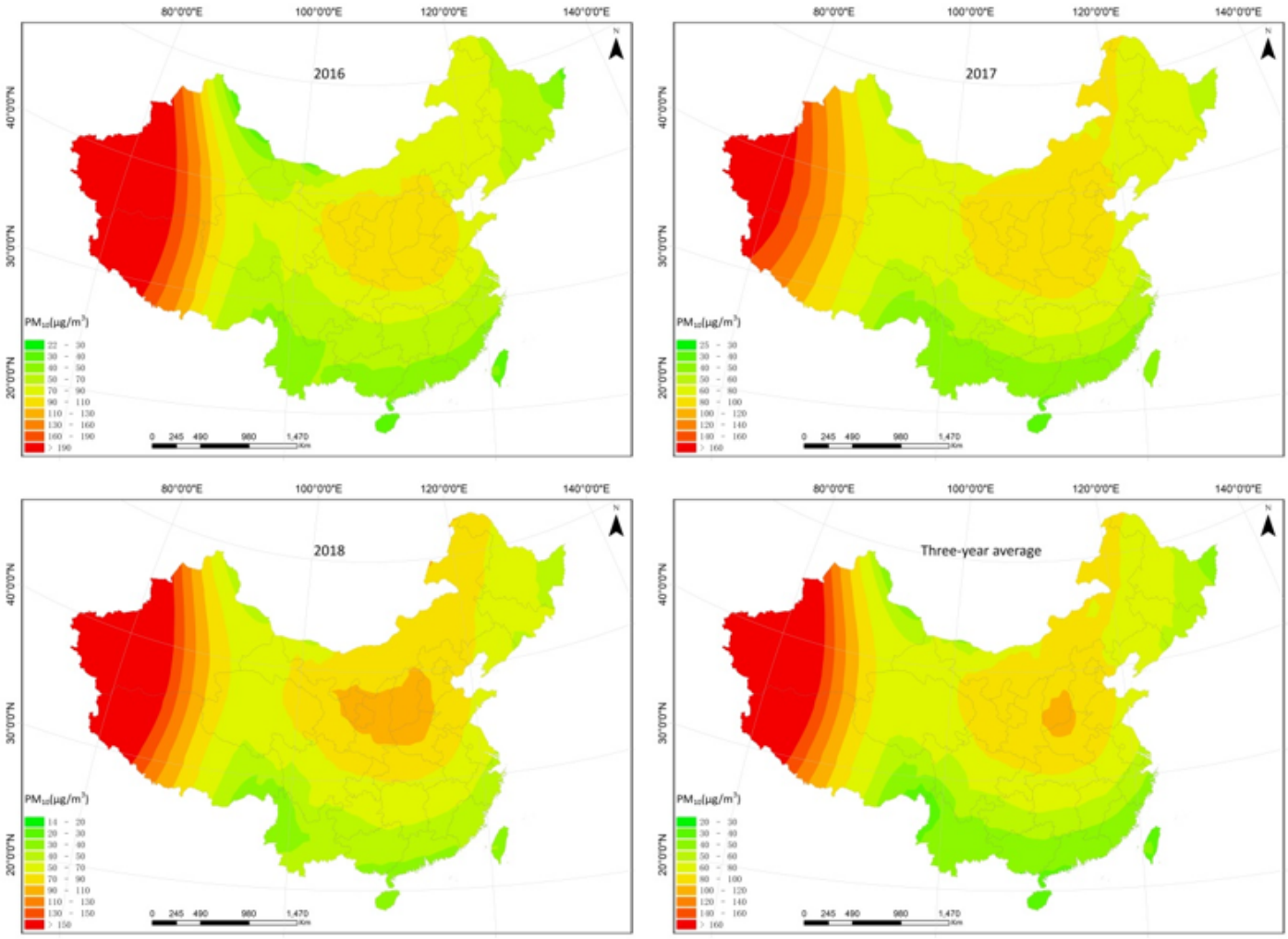

Figure 9

Spatial distribution of PM_{10} concentrations from 2016 to 2018

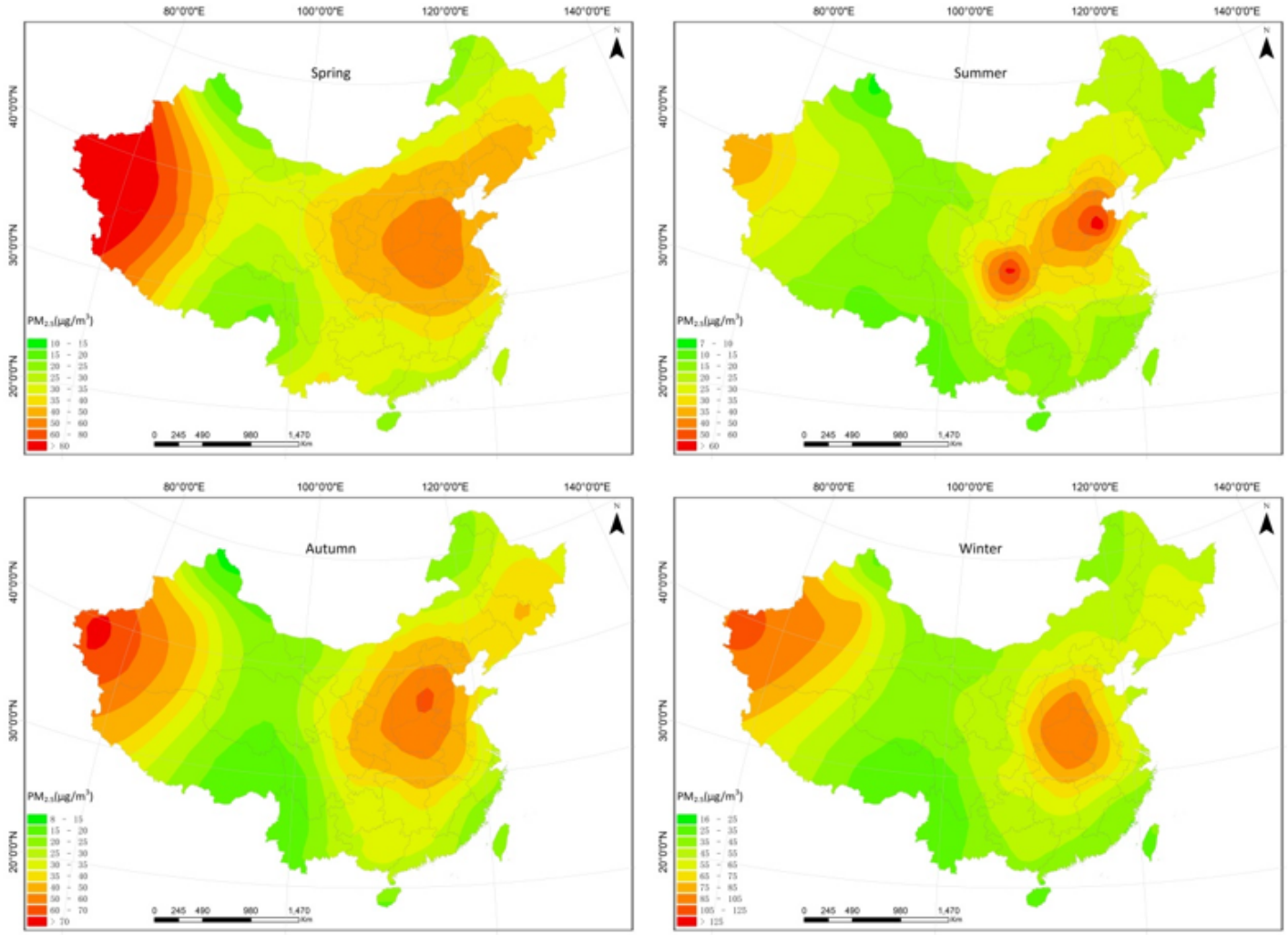

Figure 10

Spatial distribution of the average seasonal $PM_{2.5}$ concentration from 2016 to 2018

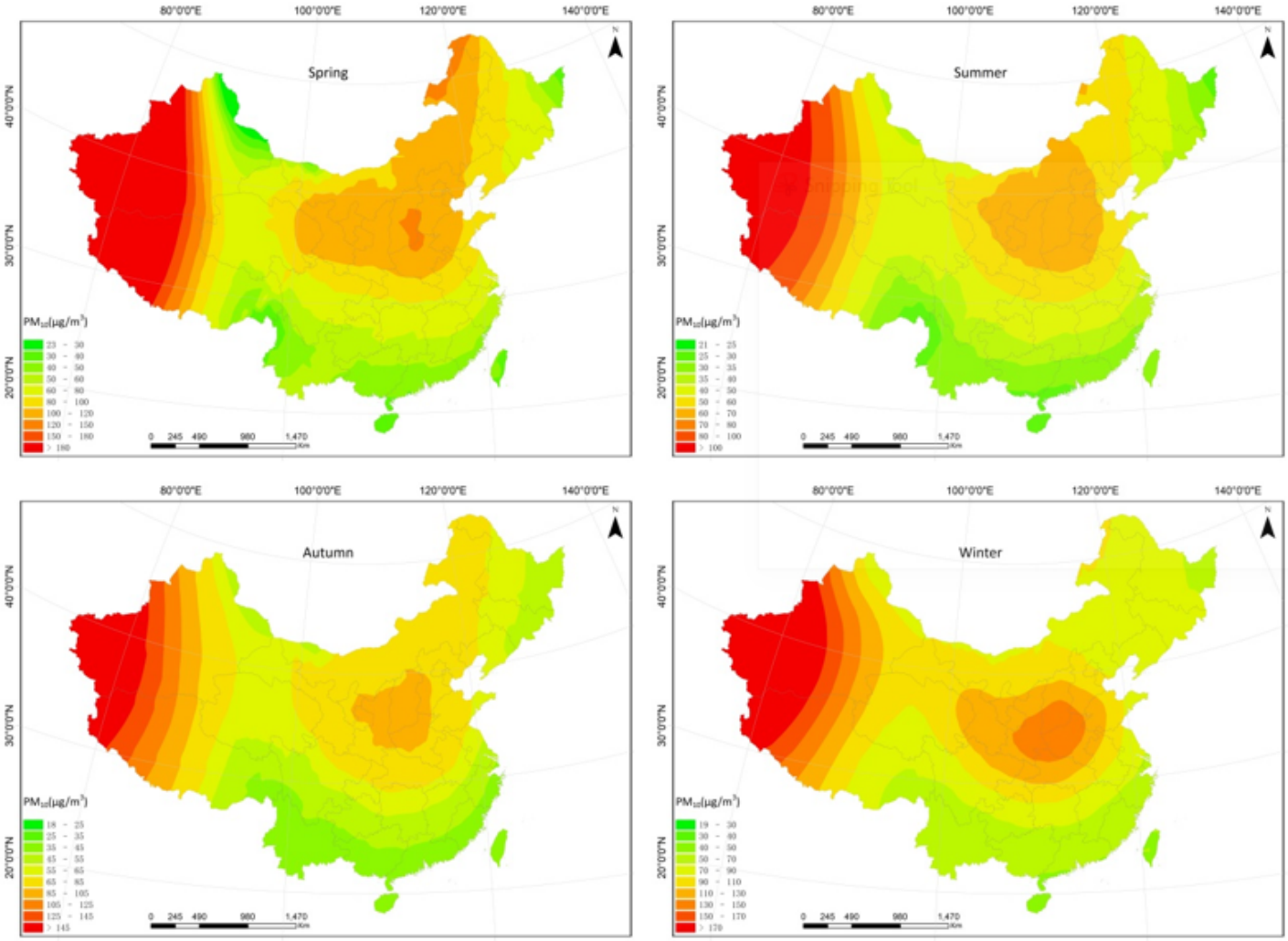

Figure 11

Spatial distribution of the average seasonal PM_{10} concentration from 2016 to 2018

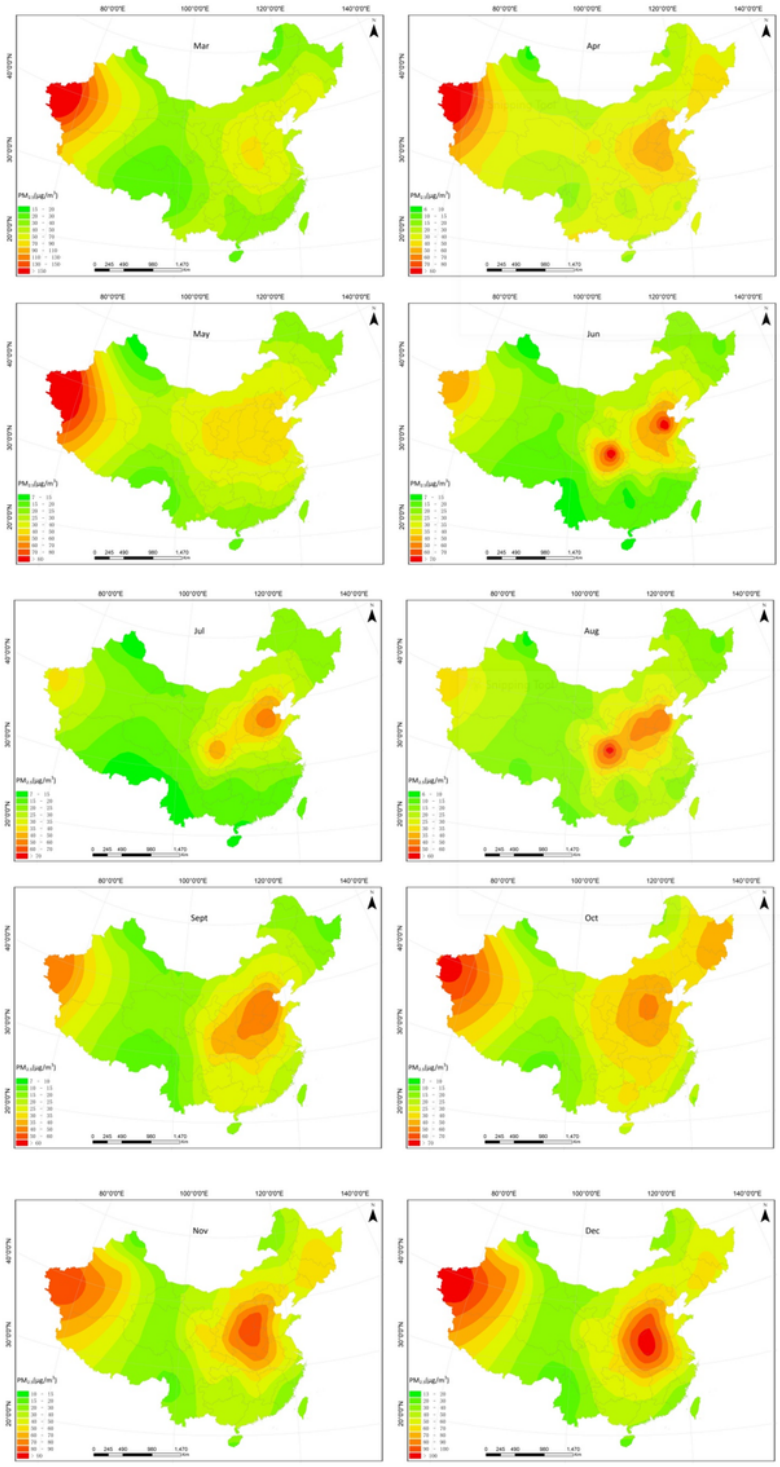

Figure 12

Spatial distribution of monthly average $PM_{2.5}$ concentrations from 2016 to 2018

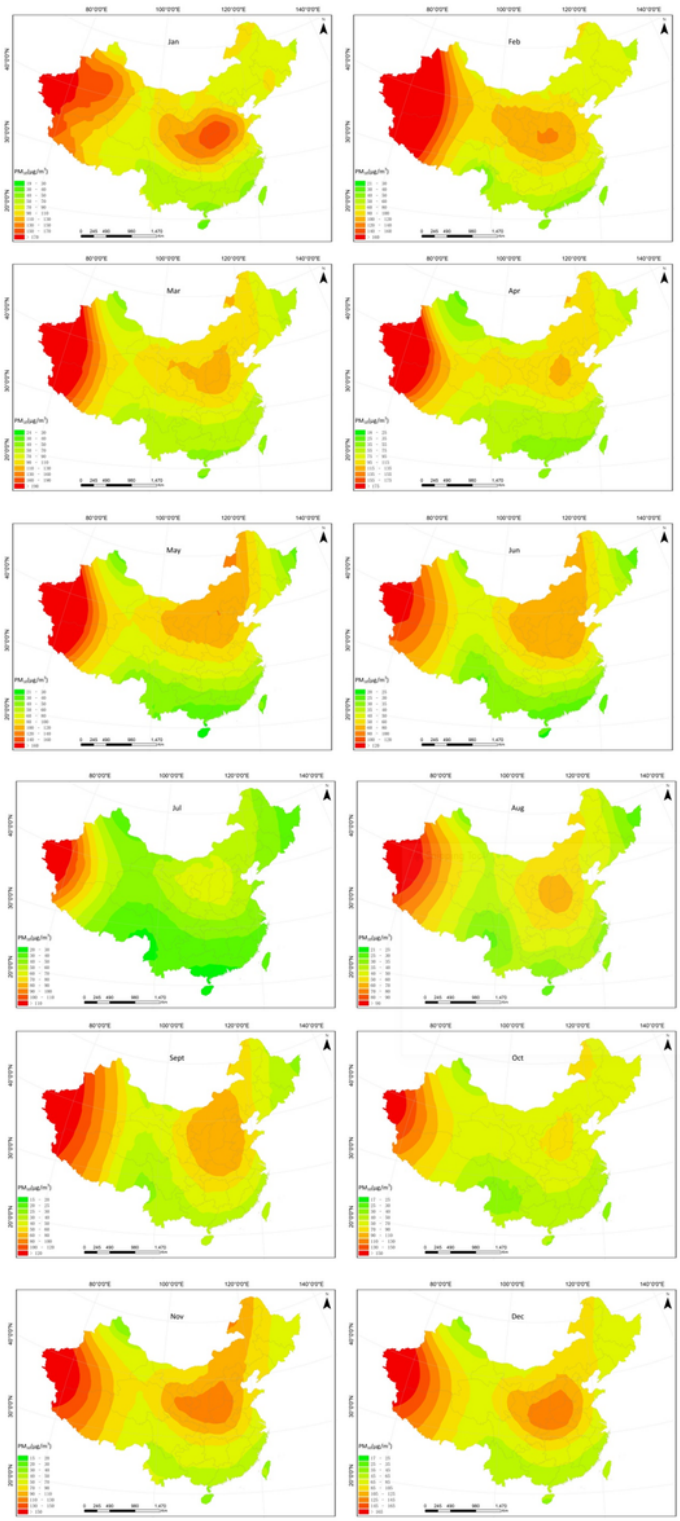

Figure 13

Spatial distribution of monthly average PM_{10} concentrations from 2016 to 2018